Polymer-Functionalized Nanodiamond Platforms as Vehicles for Gene Delivery

Xue-Qing Zhang,[†] Mark Chen,[‡,§] Robert Lam,[⊥] Xiaoyang Xu,[§] Eiji Osawa,[∥] and Dean Ho*[,†,⊥,#]

[†]Department of Biomedical Engineering, , [‡]Department of Biological Sciences, , [§]Department of Chemistry, and, [⊥]Department of Mechanical Engineering, Northwestern University, Evanston, Illinois 60208, [∥]NanoCarbon Research Institute, Shinshu University, Ueda, Nagano 386-8567, Japan, and [#]Robert H. Lurie Comprehensive Cancer Center, Northwestern University, Chicago, Illinois 60611

ABSTRACT Gene therapy holds great promise for treating diseases ranging from inherited disorders to acquired conditions and cancers. Nonetheless, because a method of gene delivery that is both effective and safe has remained elusive, these successes were limited. Functional nanodiamonds (NDs) are rapidly emerging as promising carriers for next-generation therapeutics with demonstrated potential. Here we introduce NDs as vectors for *in vitro* gene delivery *via* surface-immobilization with 800 Da polyethyleneimine (PEI800) and covalent conjugation with amine groups. We designed PEI800-modified NDs exhibiting the high transfection efficiency of high molecular weight PEI (PEI25K), but without the high cytotoxicity inherent to PEI25K. Additionally, we demonstrated that the enhanced delivery properties were exclusively mediated by the hybrid ND—PEI800 material and not exhibited by any of the materials alone. This platform approach represents an efficient avenue toward gene delivery *via* DNA-functionalized NDs, and serves as a rapid, scalable, and broadly applicable gene therapy strategy.

KEYWORDS: nanodiamonds · gene delivery · nanocarrier · transfection · low molecular weight polyethyleneimine (LMW PEI)

The purpose of gene therapy is to introduce foreign genetic material into host cells to either supplement aberrant genes or endow additional biological functions.[1] To date, however, there has been only modest progress toward this goal, mainly due to the lack of safe, broadly applicable delivery methods. There are two main approaches to gene delivery: viral and nonviral. Viral delivery is the more conventional approach because viruses have evolved to infect cells with high efficacy. As of July 2007, there have been over 1300 gene therapy clinical trials, 70% of which have used viral vectors.[2] Despite some success with viral vectors, there are still no FDA-approved products. Moreover, clinical trials have highlighted the safety risks of gene therapy *via* viral vectors as cancer and death have resulted in some cases.[3,4] In contrast, synthetic nonviral gene delivery systems, such as liposomes and polymers, offer several advantages including ease of production and reduced risk of cytotoxicity and immunogenicity,[5,6] but their use has been challenged by relatively low transfection efficiencies. This problem mainly stems from the difficulty in controlling their properties at the nanoscale, prompting the search for new modalities with better transfection efficiencies. Lately, nanocarriers have received attention in the gene therapy community including such notable examples as polyethyleneimine conjugated gold nanoparticles[7] and multifunctional nanorods.[1] Recent studies on diamond nanoparticles, also referred to as nanodiamonds (NDs), have revealed NDs as attractive platform nanocarriers due to their innate biocompatibility,[8] scalability, precise particle distribution, high surface area-to-volume ratio, near-spherical aspect ratio, and easily adaptable carbon surface for bioagent attachment.[9] NDs have been functionalized with a range of therapeutics, proteins, antibodies, DNA, polymers, and other assorted biological agents.[10−14] Furthermore, NDs are stable and dispersible in water, making them a promising and clinically important modality in improving the efficacy of the treatment of diseases and even some cancers at the molecular level. Mitochondrial function (MTT) and luminescent ATP production assays have demonstrated that NDs are not toxic to a wide variety of cell types.[15] Compared to other carbon-based nanomaterials such as CNTs, which have been shown to be toxic in many studies and are naturally not water-soluble, it is envisaged that NDs can serve as enhanced, versatile nanocarriers to deliver genes of interest in biological systems.

To rationally design a therapeutic gene delivery vector, important lessons may be learned from examining the mechanisms of gene delivery *via* proven vectors such as PEI. PEI, a polycation introduced for transfection,[16−18] is able to bind to DNA *via*

*Address correspondence to d-ho@northwestern.edu.

Received for review July 24, 2009 and accepted August 19, 2009.

Published online August 31, 2009. 10.1021/nn900865g CCC: $40.75

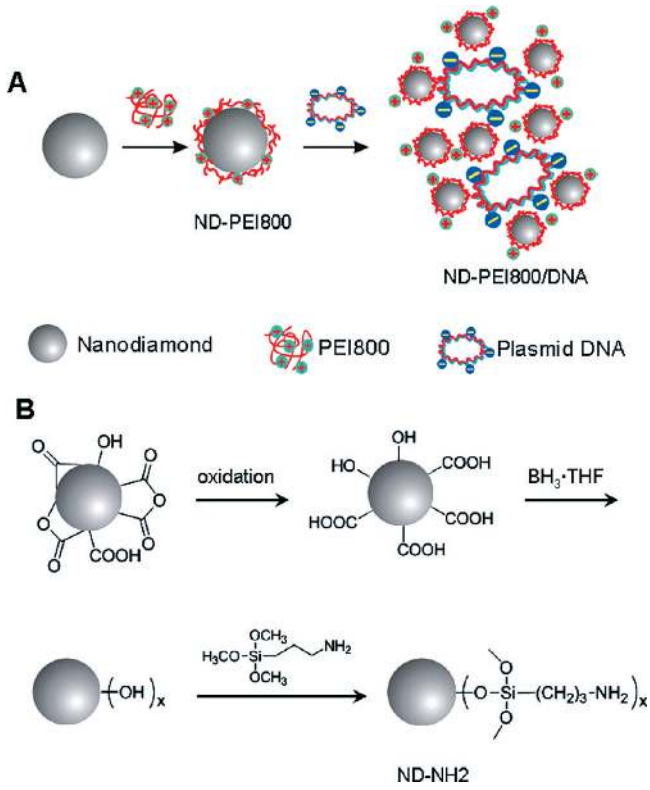

Figure 1. Schematic of (A) ND−PEI800 and (B) ND−NH_2 modification.

electrostatic interactions, protect the DNA from degradation, and is hypothesized to disrupt endosomal intake through the proton sponge effect thereby enhancing DNA delivery efficiency.[19] The transfection efficiency and toxicity of PEI correlate strongly with its molecular weight.[20] For example, low molecular weight (LMW) PEI is some 2 orders of magnitude less efficient than its 25 kDa counterpart at the same concentration, presumably because of its inability to condense DNA effectively.[21,22] Additionally, LMW PEI exhibits much lower cytotoxicity compared to its high molecular weight (HMW) analogues. Moreover, previous studies have shown that cross-linked LMW PEI could enhance gene transfer without compromising its low cytotoxicity.[21,22]

So far, many experiments have been carried out with surface-modified NDs, e.g., poly-L-lysine-coated diamonds, to explore the biological applications of NDs in DNA oligonucleotide binding[23] and biological imaging.[24] The gene delivery capacity of functional NDs has not yet been reported. In this study, we functionalized NDs with amine groups *via* either covalent attachment of (3-aminopropyl)trimethoxysilane or surface immobilization of 800 Da polyethyleneimine (PEI800) for plasmid DNA delivery. The delivery approach described in this report combines complementary characteristics of PEI800 and NDs to create a hybrid material that possesses both the low cytotoxicity of LMW PEI and the high transfection efficiency of HMW PEI. As such, the ND−PEI800 composite possesses low cytotoxicity and high transfection efficiency, properties that neither material possesses alone. This methodology is both facile and scalable and, therefore, holds promise for a wide variety of therapeutic applications in that it permits the flexible use of assorted genes and, most importantly, provides both a safe and efficient avenue for gene therapy.

In addition to NDs, a broad range of nanomaterials holds great promise and intense interest in the areas of diagnosis and therapy.[25−33] Numerous studies have been conducted to develop novel nanomaterials for biomedical and biotechnological applications, e.g., cellular tracking and imaging *via* fluorescent NDs,[27,34] functionalized single-walled carbon nanotubes[25,35] and nanohorns[36] for therapeutic agent delivery, specific targeting of glycoproteins by functionalized NDs,[37] gold nanoparticles,[29] gold nanocages,[38] and gold nanorods[33] for tumor detection and therapy, silicon nanowire,[39] quantum dot-based biosensors,[32,40−45] and platforms for fundamental investigation,[46−48] etc. Carbon-based nanomaterials, in particular, such as NDs, are attracting an increasing level of attention as they are chemically/biologically inert but can be surface functionalized for grafting of nucleic acids, peptides, proteins, and anticancer drugs. This would allow their use in the delivery of therapeutically active molecules, reducing side effects and complications.

RESULTS AND DISCUSSION

Nanodiamond−DNA Functionalization. Here we introduce functionalized ND surfaces for gene delivery *via* two modifications: noncovalent and covalent attachment. As shown in Figure 1A, 800 Da PEI was easily adsorbed to the NDs yielding ND−PEI800 since oxidized ND surfaces are prone to polar interactions such as hydrogen bonding and electrostatic interactions.[49,50] As aforementioned, PEI800 is nontoxic due to its low molecular weight, whereas its chemical structure would endow NDs with a high amino group surface density in addition to the buffering capacity that is assumed to aid in destabilization of endosomes. Negatively charged DNA was then surface immobilized onto positively charged ND−PEI800 *via* electrostatic interactions. The FTIR spectrum of ND−PEI800 was similar to that of PEI800. The peaks at 3330, 2940, 2850, and 1590 cm^{-1}, respectively, as indicated with the lines in Figure 2A, can be clearly assigned to the PEI800. Elemental analysis revealed that about 9.4 mmol of amine groups was present per gram of ND−PEI800. Additionally, TEM images of ND−PEI800 samples before and after DNA binding clearly showed that the material consists of small and evenly sized diamond nanoparticles with little to no graphitic surface coverage (Figure 2B,C). Thus, ND−PEI800 exists in the form of nanoscale agglomerates. Our second modification was the synthesis of ND−NH_2 *via* covalent attachment of (3-aminopropyl)-trimethoxysilane (Figure 1B). The carbonyl functions were reduced to hydroxymethyl groups in the pres-

ence of borane, followed by silanization using (3-aminopropyl)trimethoxysilane. The signal for C═O bonds at 1710 cm^{-1} disappeared after the reaction (Figure 2A). IR features such as the N−H vibrations at 3380 and 1630 cm^{-1}, and the C−H stretch of 2920 and 2850 cm^{-1}, confirm covalent attachment of amine groups. Elemental analysis suggested that about 0.94 mmol of amino groups was present per gram of ND−NH_2.

Dynamic light scattering (DLS) was performed to determine the average size and ζ potential of ND, ND−PEI800, and ND−NH_2 particles. Unmodified NDs form clusters with an average size of 50 nm. The covalent amino conjugation only slightly increased the particle size of NDs. Relative to ND and ND−NH_2, ND−PEI800 showed a 2-fold increase in size, suggesting PEI functionalization makes NDs more prone to agglomeration (Figure 3A). Both ND−NH_2 and ND−PEI800 had significantly higher surface potentials than unmodified ND at neutral pH (Figure 3B). Positively charged NDs were able to form complexes with pDNA *via* electrostatic interaction, and this interaction exhibited a typical weight ratio-dependent relationship. Aggregation occurred at a weight ratio of 5 for both modified NDs (Figure 3C), which is likely due to the fact that ND and ND−PEI800 have nearly neutral surfaces at weight ratio close to 5 (Figure 3D). As weight ratio increased, the particle sizes of the ND and ND−PEI800 complexes decreased to a plateau of about 100−200 nm. As expected, the net surface charge of modified ND particles increased from negative to positive as the weight ratio increased, and their ζ potentials reached a plateau of about 35−45 mV at or above weight ratio 10. Unmodified ND showed a much weaker interaction with pDNA compared to both modified ND particles. After DNA binding, the occurrence of severe aggregation was delayed to weight ratio 15, and particle sizes reached a plateau of about 100 nm up to weight ratios as high as 30. ζ potentials of ND/DNA did not reach positive values until the weight ratio increased above 17 and remained less positive than both surface functionalized ND particles.

Nanodiamond Internalization. Flow cytometry data of rhodamine-labeled ND particles incubated with HeLa cells confirmed that HeLa cells effectively internalize ND particles (Figure S1, Supporting Information). Percentage uptake by HeLa cells was found to be both concentration and time dependent. In comparison with unmodified NDs, enhanced cellular internalization of ND particles was observed after surface functionalization *via* both noncovalent PEI800 adsorption and covalent amino conjugation. These events indicated that surface functionalization is critical because particles with more positive surface potential could more efficiently interact with the plasma membrane, which presents plenty of negatively charged proteins. At the higher concentrations tested (60 μg/mL), the

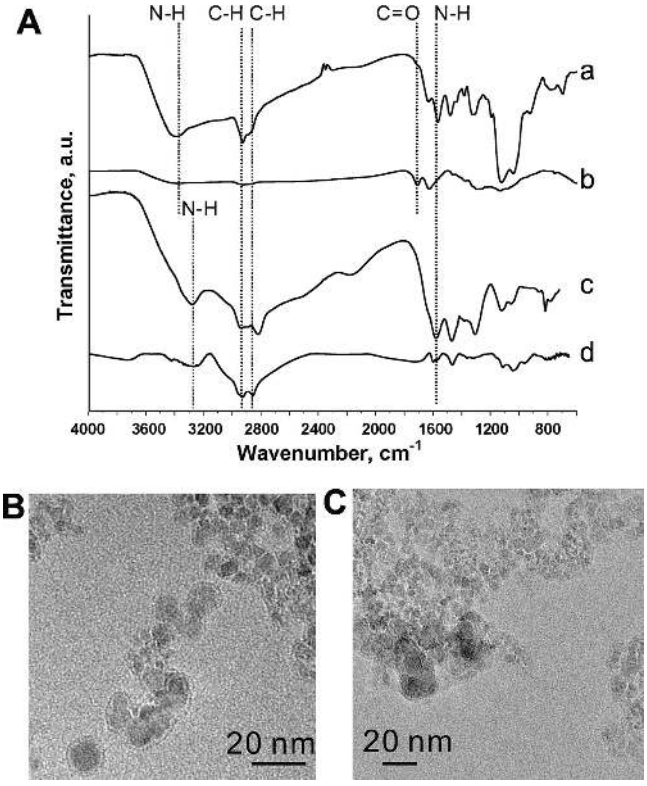

Figure 2. (A) FTIR spectra of ND−NH_2 (a), ND (b), ND−PEI800 (c), and PEI800 (d). TEM images of ND−PEI800 before (B) and after (C) DNA binding at a weight ratio of 15. Scale bars are 20 nm.

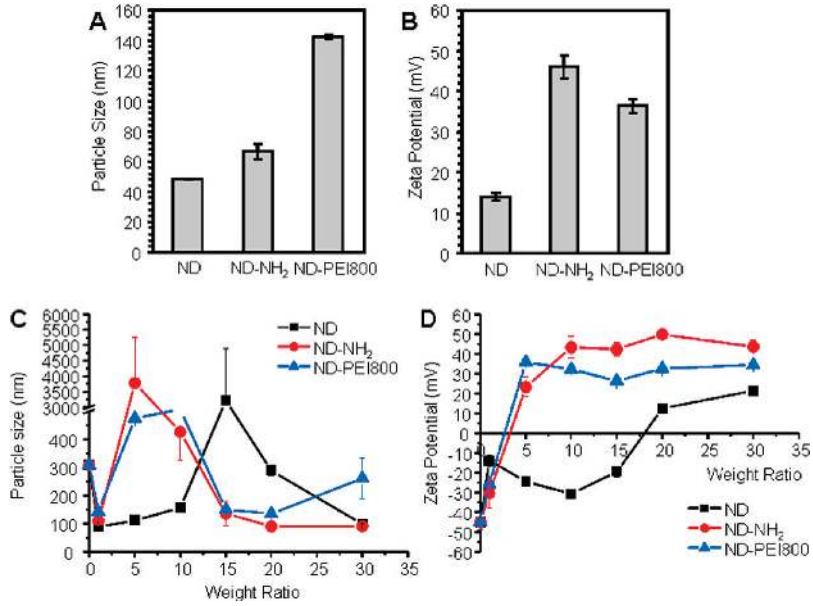

Figure 3. Size (A) and ζ potential (B) of NDs and functionalized NDs before pDNA binding. The particles were suspended in deionized water at a concentration of 60 ug/mL. Size (C) and ζ potential (D) of NDs and functionalized NDs after pDNA binding with a fixed pDNA concentration of 3 μg/mL. Data are represented as the mean ± standard deviation (N = 2).

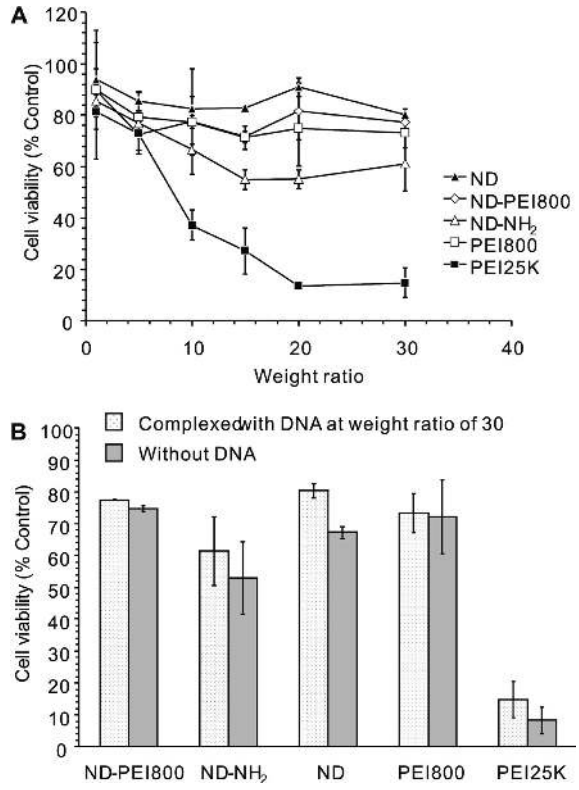

Figure 4. Cytotoxicity assay of HeLa cultures with (A) complexes formed by different carriers with pDNA at weight ratios from 1 to 30; (B) carriers (90 μg/mL) with and without pDNA at a weight ratio of 30. Data are represented as the mean ± standard deviation ($N = 4$).

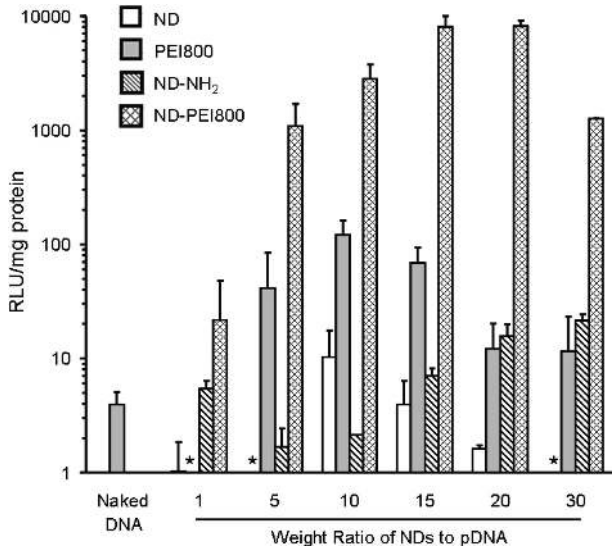

Figure 5. ND−PEI800-mediated pLuc transfection in HeLa cells induces greatest pLuc expression. Maximum transfection efficiency was observed at a weight ratio of 20 for ND−PEI800. Note the low transfection efficiency of ND alone and PEI800 alone compared to the ND−PEI800 vector. Data is represented as a mean ± standard deviation ($N = 2$). An asterisk denotes particles with transfection efficiency lower than 1 RLU/mg of protein in the cell lysate.

percentage of HeLa cells that had taken up nanoparticles increased to about 50% for both cases of ND−PEI800 and ND−NH_2 by 5 h of incubation.

Characterization of Nanodiamond−Polyethyleneimine Cytotoxicity. *In vitro* cytotoxicity of different ND carriers was evaluated in HeLa cells compared with PEI800 and 25k Da polyethyleneimine (PEI25K) by MTT assay. All ND−DNA complexes exhibited good biocompatibility (Figure 4A). Specifically, over 80% of cells survived when incubated with ND, ND−PEI800, and PEI800 complexes at weight ratios as high as 30, which corresponded to 90 μg/mL of ND or ND−PEI800 in medium. In contrast, PEI25K−DNA exhibited high cytotoxicity with cell viability decreasing as the weight ratio increased. Explicitly, less than 40% of cells were viable when incubated with PEI25K/DNA at weight ratios as low as 10, which corresponded to 30 μg/mL of PEI25K in medium. Compared to PEI25K, DNA complexes of all NDs and PEI800 only showed low to moderate cytotoxicity. The reasons for the moderate cytotoxicity induced by complexes are not fully understood, but may be attributed to the following factors. In the case of PEI800, micrometer-sized complexes were detected on the surface of the plasma membrane. It has been suggested that the deposition of such large clusters may impair plasma membrane functions and induce cell death.[20] An additional source of cellular dysfunction and cytotoxicity may arise from carrier-induced disruptions of the nucleus. It is worth noting that the cytotoxicity of all ND and PEI carriers slightly decreased when complexed with plasmid DNA (Figure 4B).

Nanodiamond-Luciferase Plasmid (pLuc) and Nanodiamond−GFP Plasmid (pEGFPLuc) Transfection Efficiency. Transfection experiments were performed using HeLa cells with all three ND carriers (Figure 5). HeLa cells have been widely used as a standard platform to model and test gene transfection efficiency and carrier-based biocompatibility. As such, successful transfection and minimal cytotoxicity were tested within the same cell line. ND/pLuc complexes formed at weight ratios ranging from 1 to 30 were included in this initial screening, and the optimal weight ratio in each case was determined. The transfection efficiencies varied as a function of the ND/pLuc weight ratio and declined in the following order: ND−PEI800 > PEI800 > ND−NH_2 > ND > naked DNA. Specifically, ND−PEI800 showed the most efficient transfection in HeLa cells and was 400 and 800 times more efficient than ND−NH_2 and unmodified ND, respectively. We hypothesize that the high amino density and buffering capacity of the cross-linked PEI800 on NDs not only facilitate efficient condensing of the plasmid but also promote plasmid escape from endosomes to the cytoplasm. Compared with both surface functionalized ND carriers, unmodified NDs mediated a lower luciferase expression, which was likely due to the poor DNA binding capacity and low surface potential as indicated by DLS results. The transfection potency of ND−PEI800 was compared systematically with that of the parent PEI800. As desired, the PEI800 cross-linked by NDs exhibited 70 times higher transfection efficiency at

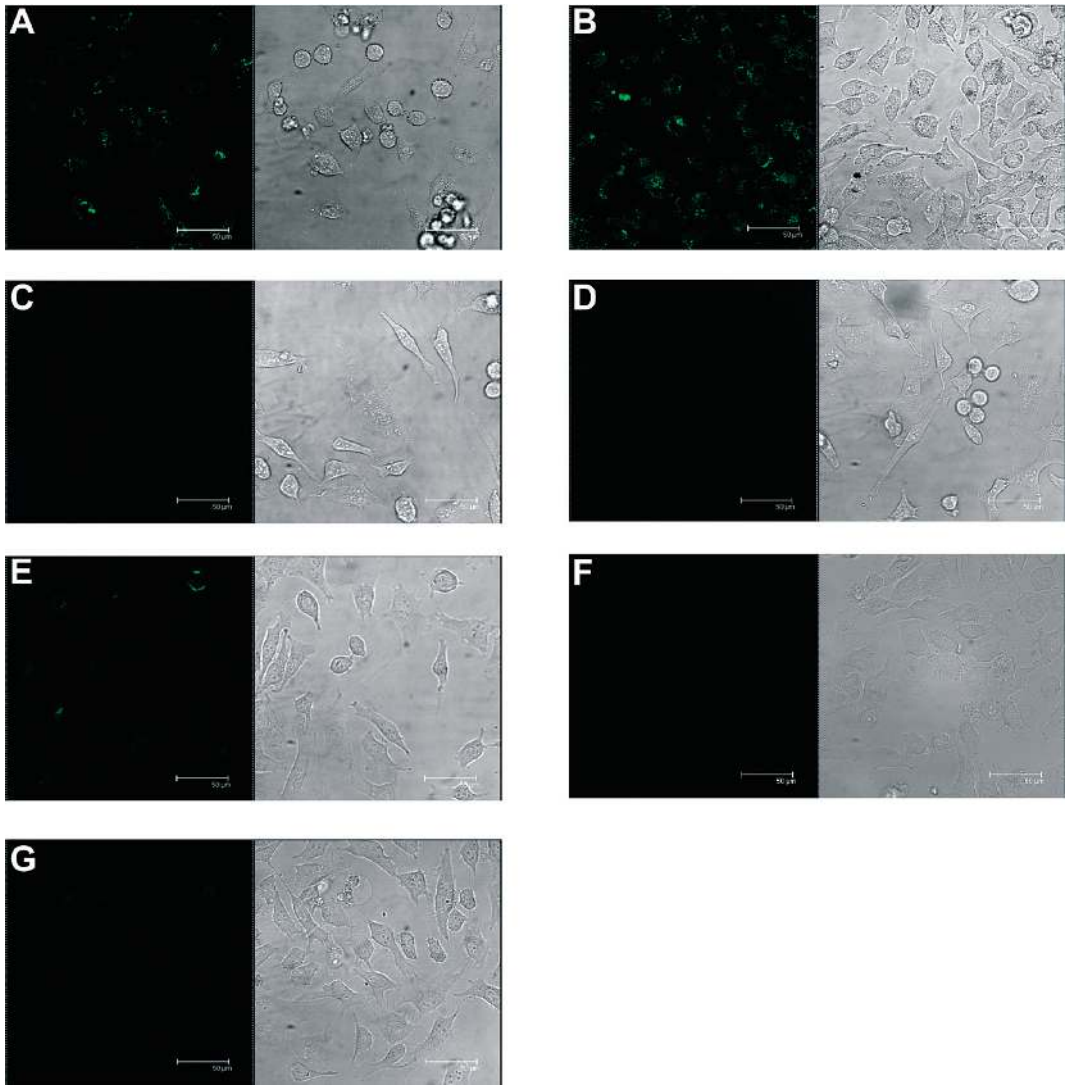

Figure 6. Confocal microscopic images of GFP expression in live HeLa cells mediated by ND−PEI800/pGFP at weight ratios of (A) 5 and (B) 15; unmodified NDs/pGFP at weight ratios of (C) 5 and (D) 15; PEI800/pGFP at weight ratios of (E) 5 and (F) 15; and (G) naked pGFP. Brightfield images are to the right of each confocal image. Scale bars are 50 μm.

the optimal weight ratio of 15 than PEI800 alone at the optimal weight ratios of 10. Although ND−PEI800 mediated a 2- to 3-fold lower luciferase expression in HeLa cells than PEI25K (data not shown), ND−PEI800 showed a much better biocompatibility than PEI25K. As demonstrated in our MTT study, more than 80% cells survived in the medium containing PEI800-functionalized NDs at concentrations as high as 90 μg/mL, whereas PEI25K killed more than 60% of cells at or above a concentration of 30 μg/mL (Figure 4A). Therefore, we have demonstrated the utility of ND−PEI800 as a potent gene delivery vector possessing both the biocompatibility of a LMW PEI and the high transfection efficiency of a HMW PEI. It is significant that neither ND nor PEI800 alone possess these positive properties.

Additionally, we examined whether ND−PEI800 could efficiently deliver and express another plasmid, pEGFPLuc encoding for GFP, in HeLa cells (Figure 6). GFP-expression could be visualized in the cytoplasm incubated with ND−PEI800/pGFP and was enhanced at higher weight ratios (Figure 6A and B). Only very weak GFP was observed in the cytoplasm when using the PEI800 or NDs as gene carriers (Figure 6C−F). Therefore, these confocal microscopy images support our conclusions derived from the quantitative luciferase expression data and demonstrate ND−PEI800 as a broadly applicable vector relevant to a spectrum of genes. HeLa cells incubated with naked DNA solution were used as a control (Figure 6G). Together with the flow cytometry and luciferase expression experiments, ND−PEI800 was further confirmed as a safe, simple, efficient gene carrier which not only facilitates the cellular internalization of the plasmid but also effectively delivers DNA to the nucleus for translation.

It is important to note that despite the successful internalization of both ND−PEI800 and ND−NH_2 particles with both possessing similar particle properties, only ND−PEI800 exhibited high transfection efficiency

(Figure 5). Regarding release of DNA, it is hypothesized that the difference in transfection efficiency between ND−PEI800 and ND−NH_2 is due to the ability of ND−PEI800 to dissociate from endosomes upon internalization. Although the exact mechanism is being explored, because the PEI800 densely coats the ND surface with amino groups, the ND−PEI800 may possess the properties of a proton sponge, which may aid in rupture of and escape from endosomes into the cytoplasm.[19] Overall, these data demonstrate that when PEI800 is added, DNA release is facilitated over time and gene expression can occur. Thus, our approach highlights the importance of rationally designed nanocarriers in overcoming the various hurdles at the many stages that lead up to gene expression.

CONCLUSION

The development of approaches toward gene therapy mediated by NDs has been rarely reported. As such, we have realized an efficient strategy for gene delivery by using low molecular weight PEI functionalized NDs and ascertained several salient features pertinent to ND-based gene delivery. While continued work investigating the mechanisms at the foundation of ND-based enhanced gene delivery is being explored, the approach presented is facile, scalable, and effective and can be extended to include other biologically relevant components that allow additional functionalities to be introduced by using the end groups present on ND surfaces. For instance, ND−PEI800 may be easily modified to incorporate such functions as cell-specific targeting or chemotherapeutic agents that are then complexed with DNA to form more complex ND-based carriers with superior performance. For these reasons, ND-based delivery may significantly improve gene therapy. Moreover, this approach may open up exciting new horizons for applications of these versatile functionalized NDs in nanomedicine.

MATERIALS AND METHODS

Materials. The 800 Da and 25 kDa PEIs, borane−tetrahydrofuran complex (BH3 · THF, 1 M), (3-aminopropyl)-trimethoxysilane, tetrahydrofuran (THF), Hoechst 33342, 5(6)-carboxy-X-rhodamine *N*-succinimidyl ester, and MTT-based cell growth determination kit were purchased from Sigma-Aldrich. The acid-oxidated ND gel (15% w/v in water) was obtained from the NanoCarbon Research Institute Ltd., Japan. All commercial reagents were used without further purification. Lysis buffer (Cell Culture Lysis Reagent 5X) and luciferase assay reagent were purchased from Promega Co. (Madison, WI). The BCA protein assay kit was purchased from Pierce (Rockford, IL). The plasmid encoding for luciferase (pNGVL1: 5.7 kb) was used for the *in vitro* luciferase transfection. The plasmid encoding for luciferase and green fluorescent protein (GFP) combined (pEGFPLuc: 5.7 kb) was used for the other *in vitro* studies including confocal microscopy, MTT assay, and DLS measurements. pEGFPLuc is a cotransfection marker that allows for normalization of transfection efficiencies by fluorescence microscopy of living cells or by a standard luciferase assay. The plasmid was transformed in *Escherichia coli* DH5α and amplified in Terrific Broth media at 37 °C overnight at 300 rpm. The plasmid was purified using an endotoxin-free QIAGEN Giga plasmid purification kit (QIAGEN, Valencia, CA) according to the manufacturer's protocol. Purified DNA was dissolved in saline, and its purity and concentration were determined by ultraviolet (UV) absorbance at 260 and 280 nm. HeLa cells were maintained in Dulbecco's minimal essential medium (DMEM) supplemented with 10% FBS, streptomycin (100 μg/mL), penicillin (100 U/mL), and 4 mM L-glutamine (ATCC, Manassas, VA) at 37 °C in a humidified 5% CO_2-containing atmosphere.

Elemental analyses were performed by Columbia Analytical Services, Inc. (Tucson, AZ). Fourier Transform Infrared Spectroscopy (FTIR) experiments were performed by using a Nexus 870 spectrometer (Thermo Nicolet, Keck-II, Northwestern University) based on OMNIC software. Transmission Electron Microscopy (TEM) was performed using a 200 kV Hitachi H-8100 TEM (EPIC, Northwestern University).

Functionalization of Nanodiamonds. Prior to use, the oxidated acid-treated NDs were diluted in deionized water at the desired concentration and ultrasonicated with a Branson 2510 sonicator (VWR International, West Chester, PA) overnight. To prepare ND−PEI800, the diluted ND solution was mixed with 800 Da PEI solution at a molar ratio of 1:10 (Figure 1A). Following two washes with deionized water, the yielding ND−PEI800 was resuspended in deionized water at a highly diluted concentration for use. ND−PEI800 samples were ultrasonicated for 5 min and immediately pipetted onto a commercial carbon TEM grid (Ted Pella Inc., Redding, CA). Upon air drying for 2 h, samples were then observed within a Hitachi H-8100 TEM. The total amount of PEI800 present in the ND−PEI800 stock solution was calculated from elemental analysis data and the weight of the solid obtained after lyophilization. Infrared spectroscopic measurements indicated the positively charged PEI800 was adsorbed onto the surface of carboxylated/oxidized NDs, covering the particles with amino groups (Figure 2A). Elemental analysis: N, 15.43; C, 57.64; H, 5.86; O, 15.49.

ND−NH_2 was synthesized according to a modified literature procedure.[9] Lyophilized ND (2 g) (elemental analysis: N, 2.22; C, 85.01; H, 1.15; O, 3.64) was finely ground and then placed in a two-necked flask under nitrogen. BH_3 · THF (20 mL, 1 M) solution in dry THF was added dropwise with stirring under reflux for 24 h. After the mixture was cooled to room temperature, hydrolysis was carried out with 2 N hydrochloric acid until no hydrogen gas evolution was observed. The solid product was isolated by centrifugation and washed with acetone and water in consecutive washing/centrifugation cycles until the supernatant liquid showed pH 7. The reduced NDs were lyophilized, and 1.1 g was added to 100 mL of a 10% solution of (3-aminopropyl)-trimethoxysilane in dry acetone under nitrogen and stirred at room temperature for 48 h. After centrifugation, the precipitate was washed with 200 mL of acetone in total in consecutive wash/centrifugation cycles and once with water yielding 982 mg of a light gray powder after lyophilization. Elemental analysis: N, 3.54; C, 81.85; H, 1.58; O, 6.64.

Rhodamine-labeled ND particles were prepared by incubating different ND particles with excess 5(6)-carboxy-X-rhodamine *N*-succinimidyl ester, respectively, in DMSO/water at room temperature for 2 h in dark. The solid products were isolated by centrifugation and washed with water in more than five washing/centrifugation cycles to remove excess reaction agents. Rhodamine-labeled ND particles were resuspended in water by ultrasonication for 2−4 h prior to use.

Cellular Internalization of Nanodiamond Carriers. HeLa cells were seeded into 24-well plates at a density of 1×10^5 cells per well in 1 mL of 10% serum-containing DMEM 24 h prior to experimentation. The media in each well was replaced with 1 mL of fresh serum-free DMEM prior to transfection. Different rhodamine-labeled ND particles were then incubated with cells at different concentrations for the desired time points. Afterward, the cells were washed with PBS, followed by incubation with 2.5 μg/mL of Hoechst 33342 for 20 min at room temperature in the dark

(counterstain). Following another PBS wash to remove excess Hoescht, cells were trypsinized and centrifuged (900 rpm, 25 °C) to remove excess trypsin-EDTA. Cells were then resuspended in 0.5 mL of PBS, and cellular uptake of nanoparticles was assessed *via* flow cytometry (BD LSR II, BD Biosciences, San Jose, CA). Dot plots were gated on FSC/SSC properties of HeLa cells to exclude free fluorescent labeled nanoparticles. Data were analyzed using BD FACSDiVa software. Quadrant markers were set accordingly using controls.

Particle Size and ζ Potential Measurements. The ND/DNA complexes were freshly prepared by mixing 3 μg of plasmid DNA with unmodified NDs, ND−NH_2, or ND−PEI800 in 1 mL of deionized water at various concentrations, corresponding to a weight ratio ranging from 0 to 30. The mixture was vortexed for 20 s and incubated for 30 min at room temperature before measurement. Particle size and ζ potential measurements were conducted using the Zetasizer Nano ZS (Malvern, Worcestershire, U.K.). The size measurements were performed at 25 °C at a 173° scattering angle. The mean hydrodynamic diameter was determined by cumulative analysis. The ζ potential determinations were based on electrophoretic mobility of the nanoparticles in the aqueous medium, which was performed using folded capillary cells in automatic mode.

Cytotoxicity Assay. The cytotoxicity of ND carriers in comparison with PEI25K was evaluated using 3-(4,5-dimethylthiazol-2-yl)-2,5-diphenyltetrazolium bromide (MTT) assay following the manufacturer's protocol. Briefly, HeLa cells were seeded in a 96-cell plate 24 h before the assay at a density of 1×10^4 cells/well. Following overnight growth, the cells were incubated for 5 h with 200 μL of DMEM medium containing respective ND/DNA complexes or PEI/DNA complexes at different weight ratios. Cells in DMEM containing 10% FBS with nothing added were used as controls. After 5 h, 20 μL of MTT solution was added to each well, and the cells were incubated for an additional 4 h. Following careful aspiration of MTT solution and media after 4 h, 200 μL of MTT solvent was added to each well and thoroughly mixed. The optical density at 570 nm was measured using a Safire microplate reader (Tecan Systems, Inc., San Jose, CA). Background absorbance at 690 nm was subtracted. Values were expressed as a percentage of the control to which no carriers had been added.

***In Vitro* Transfection and Luciferase Assay.** HeLa cells were seeded into 24-well plates at a density of 1×10^5 cells per well with 1 mL of 10% serum-containing DMEM 24 h prior to transfection. At the time of transfection, the media in each well was replaced with 1 mL of serum-free media. The complexes of ND/DNA were freshly prepared as described above. The concentrations of the unmodified ND, ND−NH_2, or ND−PEI800 nanoparticles were calculated on the basis of different weight ratios with a target pLuc dose of 3 μg/well. ND/DNA nanoparticles (100 μL) were added to the cells and incubated for 5 h at 37 °C. After 5 h, cells were washed with PBS and incubated for an additional 43 h in 1 mL of fresh serum-containing media. All transfections were performed in duplicate. After incubation, cells were washed with PBS, followed by treatment with 200 μL of 1× cell lysis buffer. The lysate was subjected to two cycles of freezing and thawing and then centrifuged at 14000 rpm for 5 min. Supernatant (20 μL) was added to 100 μL of luciferase assay reagent, and samples were measured on a TD-20/20 luminometer for 10 s (Turner Biosystems, Sunnyvale, CA). The relative light units (RLU) were normalized against protein concentration in the cell extracts, measured by a BCA protein kit. Luciferase activity was expressed as RLU/mg protein in the cell lysate. Data were reported as mean ± standard deviation for duplicate samples. Every transfection experiment was repeated twice.

Confocal Imaging of ND-Mediated GFP Expression in Live Cells. HeLa cells were seeded onto glass circular coverslips at a density of 2×10^5 cells with 2 mL of 10% serum-containing DMEM. After 24 h, transfection was undertaken with EGFP plasmid following the same protocol as for luciferase plasmid. For ND/DNA complex preparation, the concentrations of the unmodified ND, ND−NH_2, or ND−PEI800 nanoparticles were calculated on the basis of desired weight ratios with a target pEGFP dose of 6 μg/well. Live HeLa cells were viewed under a laser scanning confocal microscope (Leica Inverted Laser Scanning System, Argon Laser excitation 488 nm) 48 h after transfection.

Acknowledgment. D.H. gratefully acknowledges support from a National Science Foundation CAREER Award (CMMI-0846323), National Science Foundation Mechanics of Materials program grant (CMMI-0856492), V Foundation for Cancer Research V Scholars Award, National Science Foundation Center for Scalable and Integrated NanoManufacturing (SINAM) grant (DMI-0327077), Wallace H. Coulter Foundation Early Career Award in Translational Research, National Science Foundation National Center for Learning & Teaching in Nanoscale Science and Engineering (NCLT), and National Institutes of Health grant (U54 A1065359). M.C. appreciatively acknowledges support from the Weinberg College of Arts and Sciences of Northwestern University. We gratefully acknowledge the group of Prof. Guillermo A. Ameer for the use of their plate reader for MTT assays.

Supporting Information Available: Uptake data for rhodamine-labeled NDs in HeLa cells. This material is available free of charge *via* the Internet at http://pubs.acs.org.

REFERENCES AND NOTES

1. Salem, A. K.; Searson, P. C.; Leong, K. W. Multifunctional Nanorods for Gene Delivery. *Nat. Mater.* **2003**, *2*, 668–71.
2. Gene Therapy Clinical Trials Worldwide provided by the Journal of Gene Medicine. **2007**, www.wiley.co.uk/genmed/clinical/.
3. Hollon, T. Researchers and Regulators Reflect on First Gene Therapy Death. *Nat. Med.* **2000**, *6*, 6.
4. Check, E. Gene Therapy Put on Hold as Third Child Develops Cancer. *Nature* **2005**, *433*, 561.
5. Pouton, C. W.; Seymour, L. W. Key Issues in Non-Viral Gene Delivery. *Adv. Drug Delivery Rev.* **2001**, *46*, 187–203.
6. Green, J. J.; Langer, R.; Anderson, D. G. A Combinatorial Polymer Library Approach Yields Insight into Nonviral Gene Delivery. *Acc. Chem. Res.* **2008**, *41*, 749–759.
7. Thomas, M.; Klibanov, A. M. Conjugation to Gold Nanoparticles Enhances Polyethylenimine's Transfer of Plasmid DNA into Mammalian Cells. *Proc. Natl. Acad. Sci. U.S.A* **2003**, *100*, 9138–43.
8. Liu, K. K.; Cheng, C. L.; Chang, C. C.; Chao, J. I. Biocompatible and Detectable Carboxylated Nanodiamond on Human Cell. *Nanotechnology* **2007**, *18*, 325102.
9. Kruger, A.; Liang, Y. J.; Jarre, G.; Stegk, J. Surface Functionalisation of Detonation Diamond Suitable for Biological Applications. *J. Mater. Chem.* **2006**, *16*, 2322–2328.
10. Huang, L. C. L.; Chang, H. C. Adsorption and Immobilization of Cytochrome c on Nanodiamonds. *Langmuir* **2004**, *20*, 5879–5884.
11. Yang, W. S.; Auciello, O.; Butler, J. E.; Cai, W.; Carlisle, J. A.; Gerbi, J.; Gruen, D. M.; Knickerbocker, T.; Lasseter, T. L.; Russell, J. N.; et al. DNA-Modified Nanocrystalline Diamond Thin-films as Stable, Biologically Active Substrates. *Nat. Mater.* **2002**, *1*, 253–257.
12. Hartl, A.; Schmich, E.; Garrido, J. A.; Hernando, J.; Catharino, S. C. R.; Walter, S.; Feulner, P.; Kromka, A.; Steinmuller, D.; Stutzmann, M. Protein-Modified Nanocrystalline Diamond Thin Films for Biosensor Applications. *Nat. Mater.* **2004**, *3*, 736–742.
13. Kossovsky, N.; Gelman, A.; Hnatyszyn, H. J.; Rajguru, S.; Garrell, R. L.; Torbati, S.; Freitas, S. S.; Chow, G. M. Surface-Modified Diamond Nanoparticles as Antigen Delivery Vehicles. *Bioconjugate Chem.* **1995**, *6*, 507–511.
14. Huang, H.; Pierstorff, E.; Osawa, E.; Ho, D. Active Nanodiamond Hydrogels for Chemotherapeutic Delivery. *Nano Lett.* **2007**, *7*, 3305–3314.
15. Schrand, A. M.; Huang, H. J.; Carlson, C.; Schlager, J. J.; Osawa, E.; Hussain, S. M.; Dai, L. M. Are Diamond Nanoparticles Cytotoxic. *J. Phys. Chem. B* **2007**, *111*, 2–7.
16. Boussif, O.; Lezoualc'h, F.; Zanta, M. A.; Mergny, M. D.; Scherman, D.; Demeneix, B.; Behr, J. P. A Versatile Vector for Gene and Oligonucleotide Transfer into Cells in Culture and *in vivo*: Polyethylenimine. *Proc. Natl. Acad. Sci. U.S.A* **1995**, *92*, 7297–301.

17. Zhang, X. Q.; Tang, H. H.; Hoshi, R.; De Laporte, L.; Qiu, H. J.; Xu, X. Y.; Shea, L. D.; Ameer, G. A. Sustained Transgene Expression via Citric Acid-Based Polyester Elastomers. *Biomaterials* **2009**, *30*, 2632–2641.
18. Zhang, X. Q.; Wang, X. L.; Huang, S. W.; Zhuo, R. X.; Liu, Z. L.; Mao, H. Q.; Leong, K. W. Gene Delivery Using Polyamidoamine Dendrimers with a Trimesyl Core. *Biomacromolecules* **2005**, *6*, 341–350.
19. Akinc, A.; Thomas, M.; Klibanov, A. M.; Langer, R. Exploring Polyethylenimine-Mediated DNA Transfection and the Proton Sponge Hypothesis. *J. Gene Med.* **2005**, *7*, 657–663.
20. Fischer, D.; Bieber, T.; Li, Y. X.; Elsasser, H. P.; Kissel, T. A Novel Non-Viral Vector for DNA Delivery Based on Low Molecular Weight, Branched Polyethylenimine: Effect of Molecular Weight on Transfection Efficiency and Cytotoxicity. *Pharm. Res.* **1999**, *16*, 1273–1279.
21. Petersen, H.; Kunath, K.; Martin, A. L.; Stolnik, S.; Roberts, C. J.; Davies, M. C.; Kissel, T. Star-Shaped Poly(Ethylene Glycol)-Block-Polyethylenimine Copolymers Enhance DNA Condensation of Low Molecular Weight Polyethylenimines. *Biomacromolecules* **2002**, *3*, 926–936.
22. Gosselin, M. A.; Guo, W. J.; Lee, R. J. Efficient Gene Transfer Using Reversibly Cross-Linked Low Molecular Weight Polyethylenimine. *Bioconjugate Chem.* **2001**, *12*, 989–994.
23. Kong, X. L.; Huang, L. C. L.; Liau, S. C. V.; Han, C. C.; Chang, H. C. Polylysine-Coated Diamond Nanocrystals for MALDI-TOF Mass Analysis of DNA Oligonucleotides. *Anal. Chem.* **2005**, *77*, 4273–4277.
24. Fu, C. C.; Lee, H. Y.; Chen, K.; Lim, T. S.; Wu, H. Y.; Lin, P. K.; Wei, P. K.; Tsao, P. H.; Chang, H. C.; Fann, W. Characterization and Application of Single Fluorescent Nanodiamonds as Cellular Biomarkers. *Proc. Natl. Acad. Sci. U.S.A* **2007**, *104*, 727–732.
25. Kostarelos, K.; Lacerda, L.; Pastorin, G.; Wu, W.; Wieckowski, S.; Luangsivilay, J.; Godefroy, S.; Pantarotto, D.; Briand, J. P.; Muller, S.; et al. Cellular Uptake of Functionalized Carbon Nanotubes is Independent of Functional Group and Cell Type. *Nat. Nanotechnol.* **2007**, *2*, 108–113.
26. Lal, S.; Clare, S. E.; Halas, N. J. Nanoshell-Enabled Photothermal Cancer Therapy: Impending Clinical Impact. *Acc. Chem. Res.* **2008**, *41*, 1842–1851.
27. Chang, Y. R.; Lee, H. Y.; Chen, K.; Chang, C. C.; Tsai, D. S.; Fu, C. C.; Lim, T. S.; Tzeng, Y. K.; Fang, C. Y.; Han, C. C.; et al. Mass Production and Dynamic Imaging of Fluorescent Nanodiamonds. *Nat. Nanotechnol.* **2008**, *3*, 284–288.
28. Gobin, A. M.; Lee, M. H.; Halas, N. J.; James, W. D.; Drezek, R. A.; West, J. L. Near-Infrared Resonant Nanoshells for Combined Optical Imaging and Photothermal Cancer Therapy. *Nano Lett.* **2007**, *7*, 1929–1934.
29. Qian, X. M.; Peng, X. H.; Ansari, D. O.; Yin-Goen, Q.; Chen, G. Z.; Shin, D. M.; Yang, L.; Young, A. N.; Wang, M. D.; Nie, S. M. Tumor Targeting and Spectroscopic Detection with Surface-Enhanced Raman Nanoparticle Tags. *Nat. Biotechnol.* **2008**, *26*, 83–90.
30. Peer, D.; Karp, J. M.; Hong, S.; Farokhzad, O. C.; Margalit, R.; Langer, R. Nanocarriers as an Emerging Platform for Cancer Therapy. *Nat. Nanotechnol.* **2007**, *2*, 751–760.
31. Guan, J. J.; Lee, J. Generating Highly Ordered DNA Nanostrand Arrays. *Proc. Natl. Acad. Sci. U.S.A.* **2005**, *102*, 18321–18325.
32. Dennis, A. M.; Bao, G. Quantum Dot-Fluorescent Protein Pairs as Novel Fluorescence Resonance Energy Transfer Probes. *Nano Lett.* **2008**, *8*, 1439–45.
33. Hauck, T. S.; Jennings, T. L.; Yatsenko, T.; Kumaradas, J. C.; Chan, W. C. W. Enhancing the Toxicity of Cancer Chemotherapeutics with Gold Nanorod Hyperthermia. *Adv. Mater.* **2008**, *20*, 3832–3838.
34. Mochalin, V. N.; Gogotsi, Y. Wet Chemistry Route to Hydrophobic Blue Fluorescent Nanodiamond. *J. Am. Chem. Soc.* **2009**, *131*, 4594–4595.
35. Liu, Z.; Chen, K.; Davis, C.; Sherlock, S.; Cao, Q. Z.; Chen, X. Y.; Dai, H. J. Drug Delivery with Carbon Nanotubes for *In Vivo* Cancer Treatment. *Cancer Res.* **2008**, *68*, 6652–6660.
36. Ajima, K.; Yudasaka, M.; Murakami, T.; Maigne, A.; Shiba, K.; Iijima, S. Carbon Nanohorns as Anticancer Drug Carriers. *Mol. Pharmaceutics* **2005**, *2*, 475–480.
37. Yeap, W. S.; Tan, Y. Y.; Loh, K. P. Using Detonation Nanodiamond for the Specific Capture of Glycoproteins. *Anal. Chem.* **2008**, *80*, 4659–4665.
38. Skrabalak, S. E.; Chen, J.; Au, L.; Lu, X.; Li, X.; Xia, Y. Gold Nanocages for Biomedical Applications. *Adv. Mater.* **2007**, *19*, 3177–3184.
39. Bunimovich, Y. L.; Shin, Y. S.; Yeo, W. S.; Amori, M.; Kwong, G.; Heath, J. R. Quantitative Real-Time Measurements of DNA Hybridization with Alkylated Nonoxidized Silicon Nanowires in Electrolyte Solution. *J. Am. Chem. Soc.* **2006**, *128*, 16323–16331.
40. Zhang, C. Y.; Yeh, H. C.; Kuroki, M. T.; Wang, T. H. Single-Quantum-Dot-Based DNA Nanosensor. *Nat. Mater.* **2005**, *4*, 826–831.
41. Fu, A. H.; Gu, W. W.; Boussert, B.; Koski, K.; Gerion, D.; Manna, L.; Le Gros, M.; Larabell, C. A.; Alivisatos, A. P. Semiconductor Quantum Rods as Single Molecule Fluorescent Biological Labels. *Nano Lett.* **2007**, *7*, 179–182.
42. Alivisatos, A. P.; Gu, W. W.; Larabell, C. Quantum Dots as Cellular Probes. *Annu. Rev. Biomed. Eng.* **2005**, *7*, 55–76.
43. Fu, A. H.; Gu, W. W.; Larabell, C.; Alivisatos, A. P. Semiconductor Nanocrystals for Biological Imaging. *Curr. Opin. Neurobiol.* **2005**, *15*, 568–575.
44. Fu, A. H.; Micheel, C. M.; Cha, J.; Chang, H.; Yang, H.; Alivisatos, A. P. Discrete Nanostructures of Quantum Dots/Au with DNA. *J. Am. Chem. Soc.* **2004**, *126*, 10832–10833.
45. Alivisatos, P. The Use of Nanocrystals in Biological Detection. *Nat. Biotechnol.* **2004**, *22*, 47–52.
46. Tisler, J.; Balasubramanian, G.; Naydenov, B.; Kolesov, R.; Grotz, B.; Reuter, R.; Boudou, J.-P.; Curmi, P. A.; Sennour, M.; Thorel, A.; et al. Fluorescence and Spin Properties of Defects in Single Digit Nanodiamonds. *ACS Nano* **2009**, *3*, 1959–1965.
47. Balasubramanian, G.; Chan, I. Y.; Kolesov, R.; Al-Hmoud, M.; Tisler, J.; Shin, C.; Kim, C.; Wojcik, A.; Hemmer, P. R.; Krueger, A.; et al. Nanoscale Imaging Magnetometry with Diamond Spins under Ambient Conditions. *Nature* **2008**, *455*, 648–651.
48. Balasubramanian, G.; Neumann, P.; Twitchen, D.; Markham, M.; Kolesov, R.; Mizuoschi, N.; Isoya, J.; Achard, J.; Beck, J.; Tisler, J.; et al. Ultralong Spin Coherence Time in Isotopically Engineered Diamond. *Nat. Mater.* **2009**, *8*, 383–387.
49. Barnard, A. S.; Sternberg, M. Crystallinity and Surface Electrostatics of Diamond Nanocrystals. *J. Mater. Chem.* **2007**, *17*, 4811–4819.
50. Krueger, A. New Carbon Materials: Biological Applications of Functionalized Nanodiamond Materials. *Chem.—Eur. J.* **2008**, *14*, 1382–1390.